Scientific Correspondence

Extreme Aridity Pushes Trees to Their Physical Limits[1]

Maximilian Larter, Tim J. Brodribb, Sebastian Pfautsch, Régis Burlett, Hervé Cochard, and Sylvain Delzon*

Institut National de la Recherche Agronomique, Biodiversité, Gènes and Communautés-Unité Mixte de Recherche 1202, F–33610 Cestas, France (M.L., R.B., S.D.); Université de Bordeaux, Biodiversité, Gènes and Communautés-Unité Mixte de Recherche 1202, F–33615 Pessac, France (M.L., R.B., S.D.); School of Biological Science, University of Tasmania, Hobart, Tasmania 7001, Australia (T.J.B.); Hawkesbury Institute for the Environment, University of Western Sydney, Penrith, New South Wales 2751, Australia (S.P.); and Institut National de la Recherche Agronomique, Clermont University, Unité Mixte de Recherche 547 Physique et Physiologie Intégratives de l'Arbre Fruitier et Forestier, F–63100 Clermont-Ferrand, France (H.C.)

ORCID IDs: 0000-0002-4390-4195 (S.P.); 0000-0001-8289-5757 (R.B.); 0000-0003-3442-1711 (S.D.).

Drought-induced hydraulic failure is a leading cause of mortality of trees (McDowell et al., 2008; Anderegg et al., 2012) and has become a major concern in light of future climate predictions, with forests across the world showing signs of vulnerability to intense and prolonged drought events (Allen et al., 2010). We show here that *Callitris tuberculata*, a conifer species from extremely dry areas of Western Australia, is the most cavitation-resistant tree species in the world to date (mean xylem pressure leading to 50% loss of hydraulic function [P_{50}] = −18.8 MPa). Hydraulic conductance is maintained in these plants at pressures remarkably close to the practical limit of water metastability, suggesting that liquid water transport under the cohesion-tension theory has reached its operational boundary.

Coping with desiccation is one of the greatest challenges faced by plant life on land, and the evolution of specialized tissue for the transport of water played a key role in the colonization of continents (Black and Pritchard, 2002; Sperry, 2003). As well as evolving mechanisms to reduce water loss (e.g. stomata and waxy leaf surfaces), land plants also have to provide their aerial organs with water to fuel photosynthesis, supply metabolism, and control leaf temperature through transpiration, even when water availability is low. Driven by competition for limited resources, plants have perfected their vascular systems over hundreds of millions of years, enabling vertical transport of water to heights in excess of 100 m above the ground and resulting in the dominance of trees across a wide range of terrestrial ecosystems. However, trees are excluded from extremely dry and cold climates; we propose here that an absolute limit for water transport in trees exists, set by the physical properties of liquid water, restricting the existence of woody nonsucculent trees in dry deserts.
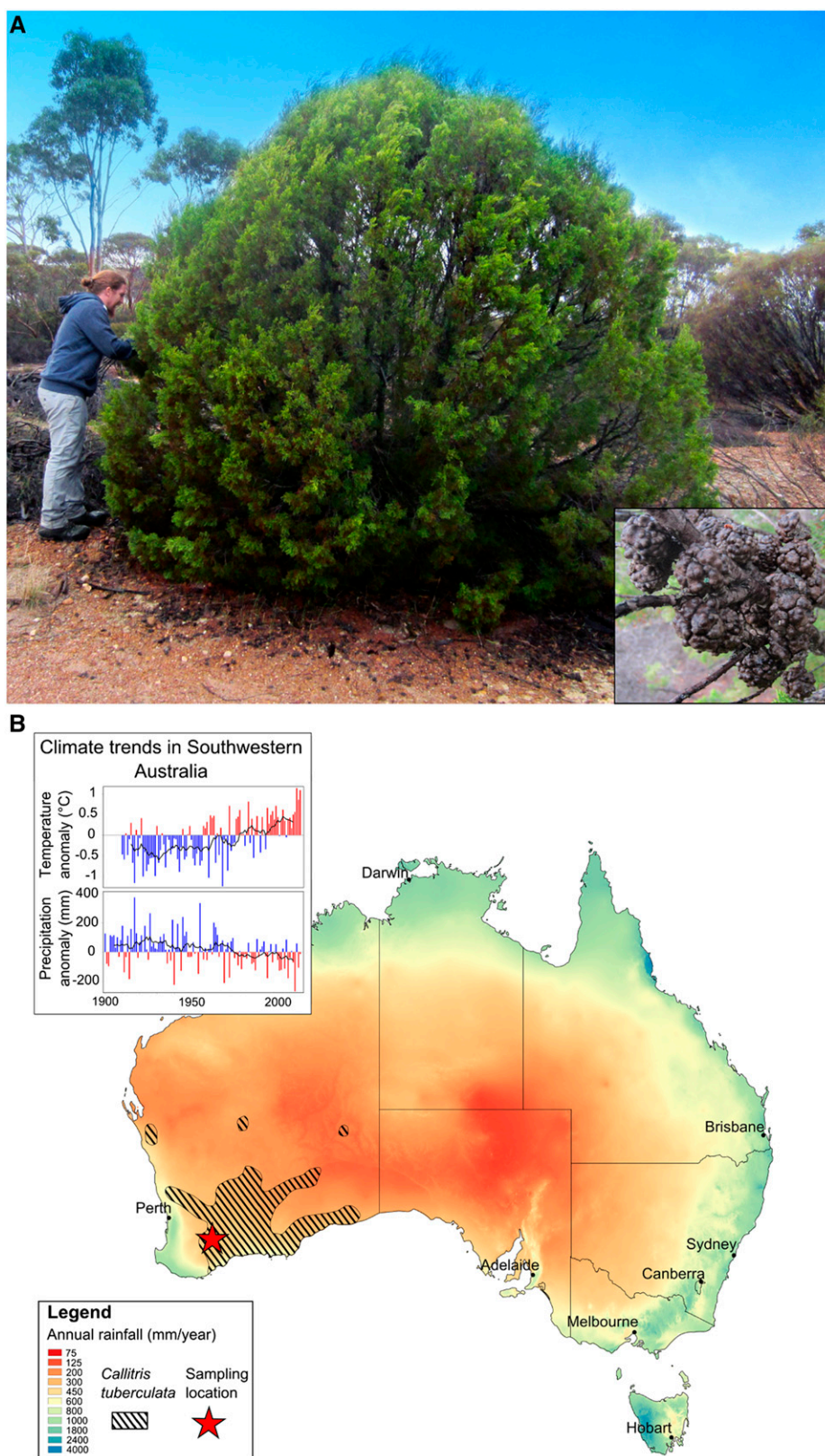
The movement of water against gravity in trees is driven by a remarkably simple process, described by the tension-cohesion theory (Tyree and Sperry, 1989; Tyree, 1997; Sperry, 2003). Evaporation at the leaf surface causes water in the plant to move up through a specialized transport tissue and drives water uptake from the soil. This leads water in the xylem to be stretched at negative pressures. However, cohesive forces due to hydrogen bonds bind water molecules together and also onto cell walls, sufficiently to maintain water in a liquid yet metastable state prone to sudden vaporization by cavitation. In moist soils, these pressures are moderate, typically above −2 MPa, but during drought, they decrease considerably, as plants are forced to extract water from drying soil, which reduces the stability of the water column. Below a specific pressure threshold, cavitation events occur when air-water menisci located at pores between xylem conduits break (Tyree, 1997; Cochard et al., 2009; Mayr et al., 2014), vaporizing sap, reducing xylem conductance, and eventually leading to plant death by desiccation (Brodribb et al., 2010; Urli et al., 2013). The xylem pressure at which cavitation occurs, leading to 50% loss of hydraulic function (P_{50}), is a trait that varies widely across species (Delzon et al., 2010; Bouche et al., 2014) and links with climate: xeric species are more resistant to cavitation than species that occupy more mesic habitats (Brodribb and Hill, 1999; Maherali et al., 2004; Choat et al., 2012; Pittermann et al., 2012). Conifers are generally more resistant to cavitation than angiosperms (Maherali et al., 2004; Choat et al., 2012), likely due to the presence of a pressure-activated safety valve that reduces the spread of air between xylem cells (Bouche et al., 2014). The most cavitation-resistant trees known

Figure 1. *C. tuberculata* appearance, distribution range, and climate. A, *C. tuberculata* from the sampled population near Lake Grace in Western Australia. The inset shows a close-up view of the tuberculate female cones of this species (photograph by A. Wesolowski). B, Map of Australia showing *C. tuberculata*'s distribution (hatched area; the red star is the sampling location). Background colors represent mean annual precipitations. The inset at top left shows annual rainfall and temperature anomalies over the 20th century compared with the average (1961–1990) for southwestern Australia. Red bars highlight hot and/or dry years, and the black line indicates the 10-year moving average.

Figure 2. Vulnerability curve for *C. tuberculata*. Points show average loss of conductance ± SE for 15 pressure classes across all individuals. The black line is the Pammenter model for the species average P_{50} (white star) and slope; the gray shaded area shows 95% confidence limits for the mean. The orange vertical line represents the maximum speed of the centrifuge. The red dashed curves and the red shaded area show bulk cavitation probability curves at 20°C, 30°C, and 40°C (from left to right). Box plots show the distribution of published P_{50} values for 384 angiosperm species (light blue) and 160 gymnosperm species (green). Outliers are detailed in the inset at top right.
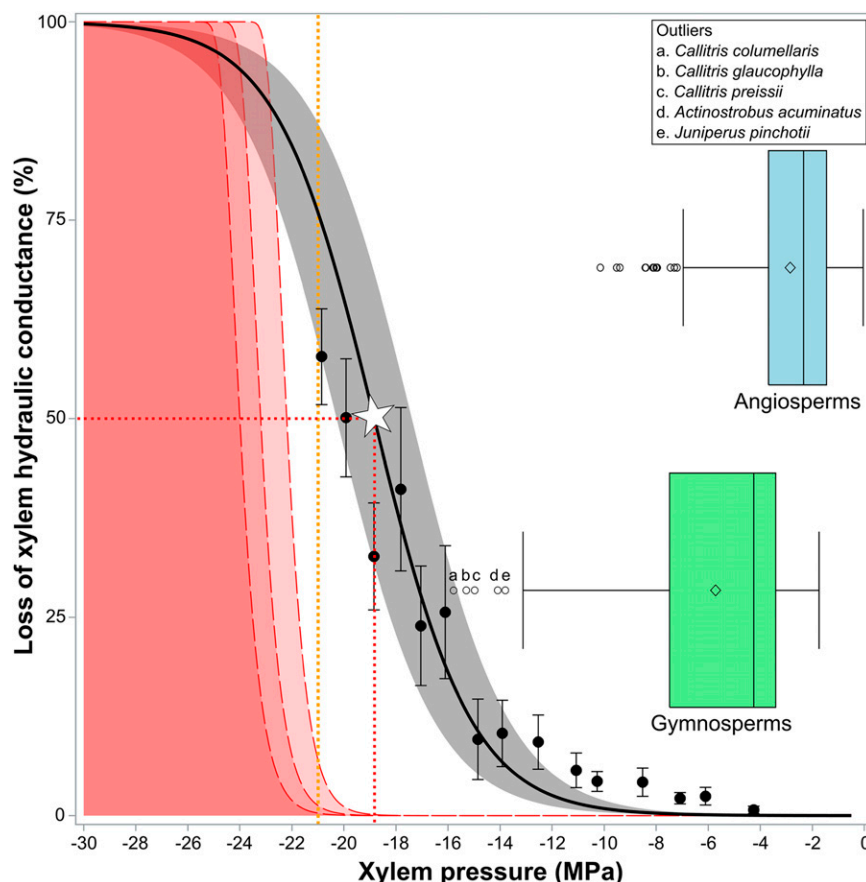
to date are conifers of the genus *Callitris* from Australia and New Caledonia, in particular *Callitris columellaris*, displaying a P_{50} of −16 MPa (Brodribb et al., 2010). Here, we present the record cavitation resistance of *Callitris tuberculata* (Cupressaceae; Fig. 1; Supplemental Materials and Methods S1). This tree species is common in extremely arid ecosystems of southwestern Australia, where its range stretches far into the Great Victoria Desert (Fig. 1B). In this area, the climate is dry and hot, with most rainfall occurring during a short wet season (Supplemental Fig. S1). At its most extreme margin, the average annual rainfall is below 180 mm, and annual evapotranspiration can exceed rainfall 10 times, presumably making this species one of the most drought-tolerant trees in the world.

Our results show that this species from the desert tree line produces a previously unparalleled P_{50} of −18.8 ± 0.6 MPa (*n* = 9; Fig. 2; Supplemental Fig. S2; Supplemental Table S1), making it, to our knowledge, the most drought-resistant tree ever measured. At −21 MPa, the lowest pressure we could achieve with our device (thus extending the experimental xylem pressure range by nearly 20%, from −17.3 MPa; Brodribb et al., 2010), around 25% to 50% of xylem conduits were still functional, with the final cavitation events predicted to occur at about −25 MPa. Could evolution push xylem pressure to more extreme values to enable this species to colonize even drier habitats? Strikingly, physics'

answer is no, as *C. tuberculata* has reached the operational limit of water metastability.

According to the classical nucleation theory (Debenedetti, 1996), homogenous water cavitation occurs at pressures below −120 MPa at ambient temperature, as has been verified by experiments using microscopic liquid water inclusions in quartz (Zheng et al., 1991; Azouzi et al., 2013). Conversely, other experimental data suggest that bulk cavitation occurs heterogenously on ubiquitous impurities at much higher pressures, from −20 to −30 MPa, depending on the method used to induce negative pressure, water purity, and water temperature (for review, see Caupin et al., 2012). Consistently, in recent experiments based on a synthetic tree (Wheeler and Stroock, 2008; Vincent et al., 2012), bulk cavitation occurs rapidly at tensions of around −22 MPa. The presence of impurities, dissolved minerals, and nutrients in xylem sap (Buhtz et al., 2004; Krishnan et al., 2011) leads us to speculate that bulk cavitation in tree xylem will likely occur at similar pressures, setting an absolute physical limit for water transport in trees during drought.

Drought stress has pushed this species to evolve the most resistant xylem, to the point that *C. tuberculata* is able to potentially maintain water flow up to the limit of physical properties of liquid water. Already growing in an environment severely limited by water availability,

its adaptation to future conditions (i.e. by lowering P_{50}) may be restricted by reaching this physical boundary. Indeed, in southwestern Australia, a strong trend toward a drier and warmer climate has been evidenced over the 20th century (Fig. 1B, inset). This could lead to a contraction of forest at the desert margin, but it also offers the possibility of a range expansion into historically wetter regions to the southwest.

Hydraulic failure is one of the main hypotheses to explain tree death following prolonged periods of drought (Anderegg et al., 2012). Experiments have shown that, after reaching cavitation levels of around 50% in conifers or 90% in angiosperms, trees cannot recover (Brodribb et al., 2010; Urli et al., 2013). Furthermore, a recent study showed that trees in all ecosystems function with similarly narrow safety margins regarding this threshold to cavitation (Choat et al., 2012). Like southwestern Australia, many regions are projected to suffer from increasingly frequent and severe droughts (Stocker et al., 2013), highlighting the need to better understand the physiological responses of trees to drought stress to improve predictions of the impact of climate change on forests and woodlands. Our results suggest that *C. tuberculata* is an ideal candidate for further investigations, for example into xylem anatomy modifications allowing the evolution of increased cavitation resistance. Evolution toward xylem safety from cavitation leads to a tolerance strategy, allowing plants to maintain limited function even in stressed conditions. We have discovered an absolute limit to this evolutionary path due to water metastability in the xylem, explaining why trees tend to be excluded from the most arid ecosystems.

Supplemental Data

The following supplemental materials are available.

Supplemental Figure S1. Climate data.

Supplemental Figure S2. Vulnerability curves for all individuals.

Supplemental Table S1. Hydraulic traits for *Callitris* spp. individuals.

Supplemental Materials and Methods S1. Detailed description of data collection and analysis.

LITERATURE CITED

Allen CD, Macalady AK, Chenchouni H, Bachelet D, McDowell N, Vennetier M, Kitzberger T, Rigling A, Breshears DD, Hogg EH, et al (2010) A global overview of drought and heat-induced tree mortality reveals emerging climate change risks for forests. For Ecol Manage **259:** 660–684

Anderegg WR, Berry JA, Smith DD, Sperry JS, Anderegg LD, Field CB (2012) The roles of hydraulic and carbon stress in a widespread climate-induced forest die-off. Proc Natl Acad Sci USA **109:** 233–237

Azouzi ME, Ramboz C, Lenain JF, Caupin F (2013) A coherent picture of water at extreme negative pressure. Nat Phys **9:** 38–41

Black M, Pritchard HW, editors (2002) Desiccation and Survival in Plants: Drying without Dying. CABI Publishing, Wallingford, UK

Bouche PS, Larter M, Domec JC, Burlett R, Gasson P, Jansen S, Delzon S (2014) A broad survey of hydraulic and mechanical safety in the xylem of conifers. J Exp Bot **65:** 4419–4431

Brodribb T, Hill RS (1999) The importance of xylem constraints in the distribution of conifer species. New Phytol **143:** 365–372

Brodribb TJ, Bowman DJ, Nichols S, Delzon S, Burlett R (2010) Xylem function and growth rate interact to determine recovery rates after exposure to extreme water deficit. New Phytol **188:** 533–542

Buhtz A, Kolasa A, Arlt K, Walz C, Kehr J (2004) Xylem sap protein composition is conserved among different plant species. Planta **219:** 610–618

Caupin F, Arvengas A, Davitt K, Azouzi MM, Shmulovich KI, Ramboz C, Sessoms DA, Stroock AD (2012) Exploring water and other liquids at negative pressure. J Phys Condens Matter **24:** 284110

Choat B, Jansen S, Brodribb TJ, Cochard H, Delzon S, Bhaskar R, Bucci SJ, Feild TS, Gleason SM, Hacke UG, et al (2012) Global convergence in the vulnerability of forests to drought. Nature **491:** 752–755

Cochard H, Hölttä T, Herbette S, Delzon S, Mencuccini M (2009) New insights into the mechanisms of water-stress-induced cavitation in conifers. Plant Physiol **151:** 949–954

Debenedetti PG (1996) Metastable Liquids: Concepts and Principles. Princeton University Press, Princeton, NJ

Delzon S, Douthe C, Sala A, Cochard H (2010) Mechanism of water-stress induced cavitation in conifers: bordered pit structure and function support the hypothesis of seal capillary-seeding. Plant Cell Environ **33:** 2101–2111

Krishnan HB, Natarajan SS, Bennett JO, Sicher RC (2011) Protein and metabolite composition of xylem sap from field-grown soybeans (Glycine max). Planta **233:** 921–931

Maherali H, Pockman WT, Jackson RB (2004) Adaptive variation in the vulnerability of woody plants to xylem cavitation. Ecology **85:** 2184–2199

Mayr S, Kartusch B, Kikuta S (2014) Evidence for air-seeding: watching the formation of embolism in conifer xylem. J Plant Hydraul **1:** e-0004

McDowell N, Pockman WT, Allen CD, Breshears DD, Cobb N, Kolb T, Plaut J, Sperry J, West A, Williams DG, et al (2008) Mechanisms of plant survival and mortality during drought: why do some plants survive while others succumb to drought? New Phytol **178:** 719–739

Pittermann J, Stuart SA, Dawson TE, Moreau A (2012) Cenozoic climate change shaped the evolutionary ecophysiology of the Cupressaceae conifers. Proc Natl Acad Sci USA **109:** 9647–9652

Sperry JS (2003) Evolution of water transport and xylem structure. Int J Plant Sci **164:** S115–S127

Stocker TF, Qin D, Plattner GK, Tignor MM, Allen SK, Boschung J, Nauels A, Xia Y, Bex V, Midgley PM (2013) IPCC, 2013: Climate Change 2013: The Physical Science Basis. Cambridge University Press, Cambridge, UK

Tyree MT (1997) The cohesion-tension theory of sap ascent: current controversies. J Exp Bot **48:** 1753–1765

Tyree MT, Sperry JS (1989) Vulnerability of xylem to cavitation and embolism. Annu Rev Plant Biol **40:** 19–36

Urli M, Porté AJ, Cochard H, Guengant Y, Burlett R, Delzon S (2013) Xylem embolism threshold for catastrophic hydraulic failure in angiosperm trees. Tree Physiol **33:** 672–683

Vincent O, Marmottant P, Quinto-Su PA, Ohl CD (2012) Birth and growth of cavitation bubbles within water under tension confined in a simple synthetic tree. Phys Rev Lett **108:** 184502

Wheeler TD, Stroock AD (2008) The transpiration of water at negative pressures in a synthetic tree. Nature **455:** 208–212

Zheng Q, Durben DJ, Wolf GH, Angell CA (1991) Liquids at large negative pressures: water at the homogeneous nucleation limit. Science **254:** 829–832

1   **Supplemental material:**

2   **Materials and Methods:**

3   **Sampling**

4   As part of investigations into record cavitation-resistant conifers, we collected samples

5   (branches of about 40 cm) from a population of *Callitris tuberculata* near Lake Grace (WA,

6   Australia) in July 2014. They were immediately wrapped in wet paper towels with foliage

7   removed, and sent for measurement at the BIOGECO lab at INRA - University of Bordeaux

8   (France; http://sylvain-delzon.com/?page_id=536) where they were kept in dark, damp and

9   refrigerated conditions until measurements were conducted.

10   **Vulnerability curves**

11   Cavitation resistance was estimated with the flow-centrifuge technique, based on the

12   Cavitron method (Cochard *et al.*, 2005), in which centrifugation is used to induce negative

13   pressure in the xylem of the sample and conductance is monitored during spinning (as

14   measured by the water flow through the stem). Samples were cut to length (27 cm), then bark

15   was removed and the ends were re-cut with a clean razor blade. We used a specially designed

16   centrifuge rotor, reinforced to allow previously unattainable speeds of above 13000 rpm. We

17   thus reached a record maximum speed of 15000 rpm, which induces xylem pressure of around

18   -21 MPa. Maximum conductance is estimated at low speed (high pressure), then we gradually

19   increase rotation speed, repeatedly measuring conductance at least 3 times at each pressure

20   step. As xylem pressure is forced to more negative values, cavitation events occur, leading to

21   a drop in hydraulic conductance, which is classically represented as so-called vulnerability

22   curves, percent loss of conductance (or PLC) as a function of pressure. Each individual

23   vulnerability curve was fit using the Pammenter model (Pammenter and Vander Willigen,

24   1998), with P_{50} derived as the pressure leading to a 50% decrease in conductance

25   (Supplemental Fig. S2). This procedure has been extensively described elsewhere, see for

26   example Methods in Delzon et al. (2010) and Jansen et al. (2012). Individual P_{50} and other

27   parameters for each individual are presented in Supplemental Table S1. Conductance

28   measurements for all individuals were pooled and binned into 15 pressure classes, to create an

29   average vulnerability curve (Fig. 1). The shaded area in Fig. 1 represents the 95% confidence

30   interval for the mean obtained with the CLM option in the Means Procedure in SAS. All

31   statistical analyses was conducted using SAS software (SAS 9.4 Institute, Cary, NC, USA).

32   This method also enables estimation of xylem specific conductivity, a measure of

33 xylem capacity to transport water. No significant correlation with xylem safety from

34 cavitation was found within this population of *C. tuberculata* (regression analysis r^2=0.035;

35 P=0.63), indicating absence of a functional trade-off between safety and efficiency.

Cavitation resistance data

37   We extracted published measurements of cavitation resistance from Choat et al. (2012)

38 and Bouche et al. (2014) of both Angiosperm and Gymnosperm species to allow comparison

39 of *Callitris tuberculata* to other species. These datasets are available online respectively from

40 the Nature and Journal of Experimental Botany websites.

Bulk cavitation curves

42   Bulk heterogeneous cavitation curves for temperatures of 20, 30 and 40°C (likely to

43 occur in the xylem of *C. tuberculata* during summer drought) were constructed based on

44 equation 12 in Herbert et al. (2006).

Climate data

46   Annual temperature and precipitation deviation from the 1961-1990 average was

47 obtained from the Australian Bureau of Meterology (http://www.bom.gov.au). *Callitris*

48 *tuberculata* occurrences were downloaded from the Global Biodiversity Information Facility

49 (GBIF; http://www.gbif.org), and used to outline an approximate distribution range. Climate

50 layers were then obtained from Worldclim (Hijmans *et al.*, 2005) (http://www.worldclim.org)

51 and the Global Aridity Index and PET datasets (http://www.cgiar-csi.org/data/global-aridity-

52 and-pet-database), and data for each location was extracted in QGIS 2.4.0 (Quantum, 2011)

53 using the point-sampling tool. We show here the average monthly precipitations and

54 maximum daily temperature for all locations obtained from GBIF (Supplemental Fig. S1).

55

56

57

58

59

60

61

62 **Literature cited :**

63 **Bouche PS, Larter M, Domec J-C, Burlett R, Gasson P, Jansen S, Delzon S**. 2014. A broad survey of
64 hydraulic and mechanical safety in the xylem of conifers. Journal of experimental botany.

65 **Choat B, Jansen S, Brodribb TJ, *et al.*** 2012. Global convergence in the vulnerability of forests to
66 drought. Nature **491**, 752–755.

67 **Cochard H, Damour G, Bodet C, Tharwat I, Poirier M, Améglio T**. 2005. Evaluation of a new
68 centrifuge technique for rapid generation of xylem vulnerability curves. Physiologia Plantarum **124**,
69 410–418.

70 **Delzon S, Douthe C, Sala A, Cochard H**. 2010. Mechanism of water-stress induced cavitation in
71 conifers: bordered pit structure and function support the hypothesis of seal capillary-seeding. Plant,
72 cell & environment **33**, 2101–2111.

73 **Herbert E, Balibar S, Caupin F**. 2006. Cavitation pressure in water. Physical Review E **74**, 041603.

74 **Hijmans RJ, Cameron SE, Parra JL, Jones PG, Jarvis A**. 2005. Very high resolution interpolated climate
75 surfaces for global land areas. International Journal of Climatology **25**, 1965–1978.

76 **Jansen S, Lamy J-B, Burlett R, Cochard H, Gasson P, Delzon S**. 2012. Plasmodesmatal pores in the
77 torus of bordered pit membranes affect cavitation resistance of conifer xylem. Plant, cell &
78 environment.

79 **Pammenter NW, Vander Willigen C**. 1998. A mathematical and statistical analysis of the curves
80 illustrating vulnerability of xylem to cavitation. Tree physiology **18**, 589–593.

81 **Quantum G**. 2011. Development Team, 2012. Quantum GIS Geographic Information System. Open
82 Source Geospatial Foundation Project. [http://qgis.osgeo.org].

83

84

85

86

87

88

89

90

91

92

93

94

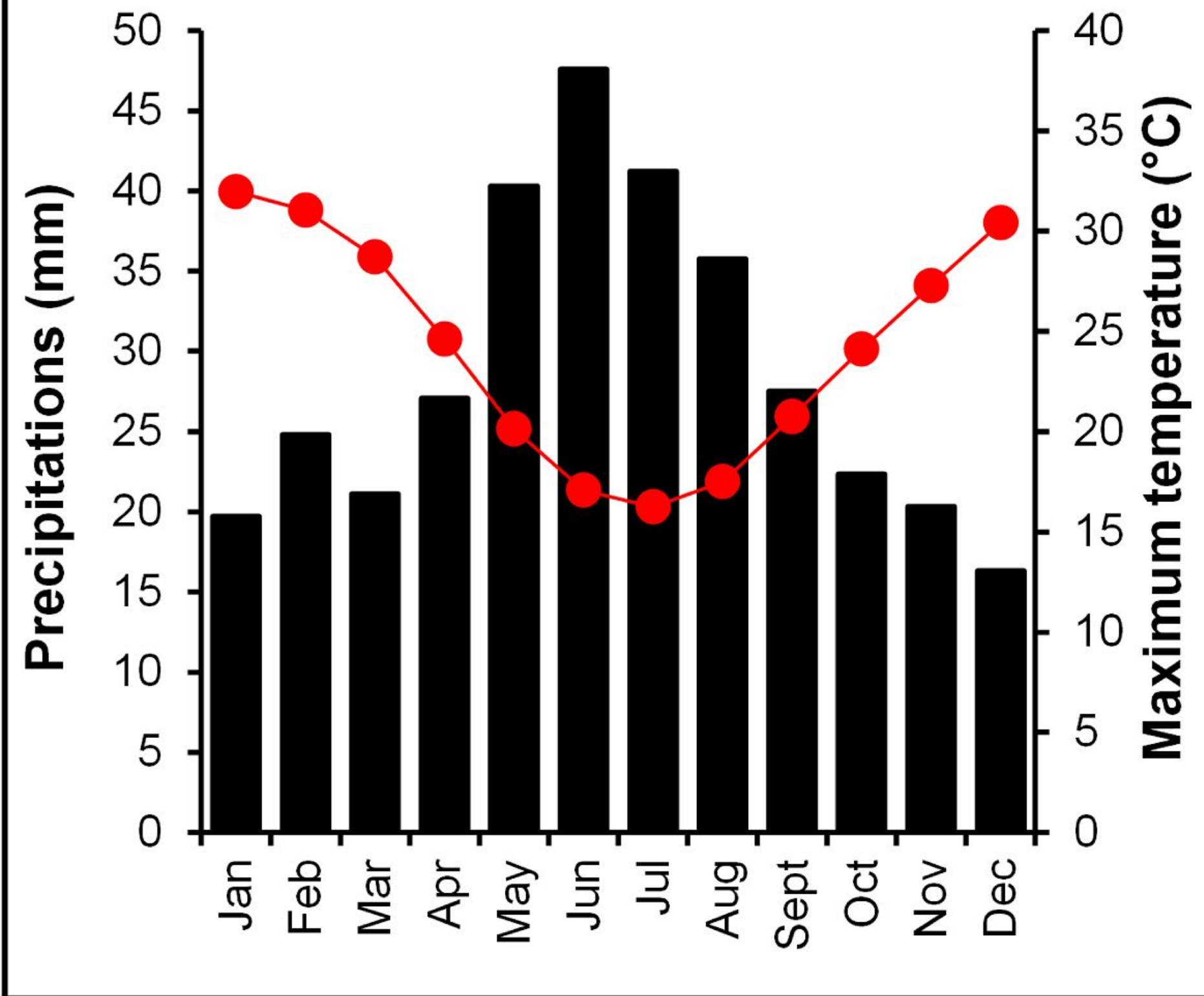3

Figure S1. Climate diagram of average monthly precipitations and maximum temperatures for *Callitris tuberculata*'s estimated range. Black bars represent monthly precipitations, and the red curve shows maximum temperatures.

Figure S2. Vulnerability curves for nine individual trees of *Callitris tuberculata*. Each point represents mean value of percent loss of hydraulic conductance over at least three measurements of hydraulic conductance (bars represent ± standard error). Lines represent the Pammenter model fit to each individual curve, and dashed lines show were the model was expanded beyond experimental data.

Table S1. Cavitation resistance parameters for each individual. P_{50}, P_{12}, and P_{88} are, respectively, the xylem pressure inducing 50%, 12% and 88% loss of xylem hydraulic conductance. *S* is the slope of the vulnerability curve at P_{50}. *ks* is the specific xylem conductivity, a standardized measurement of the samples' capacity to transport water.
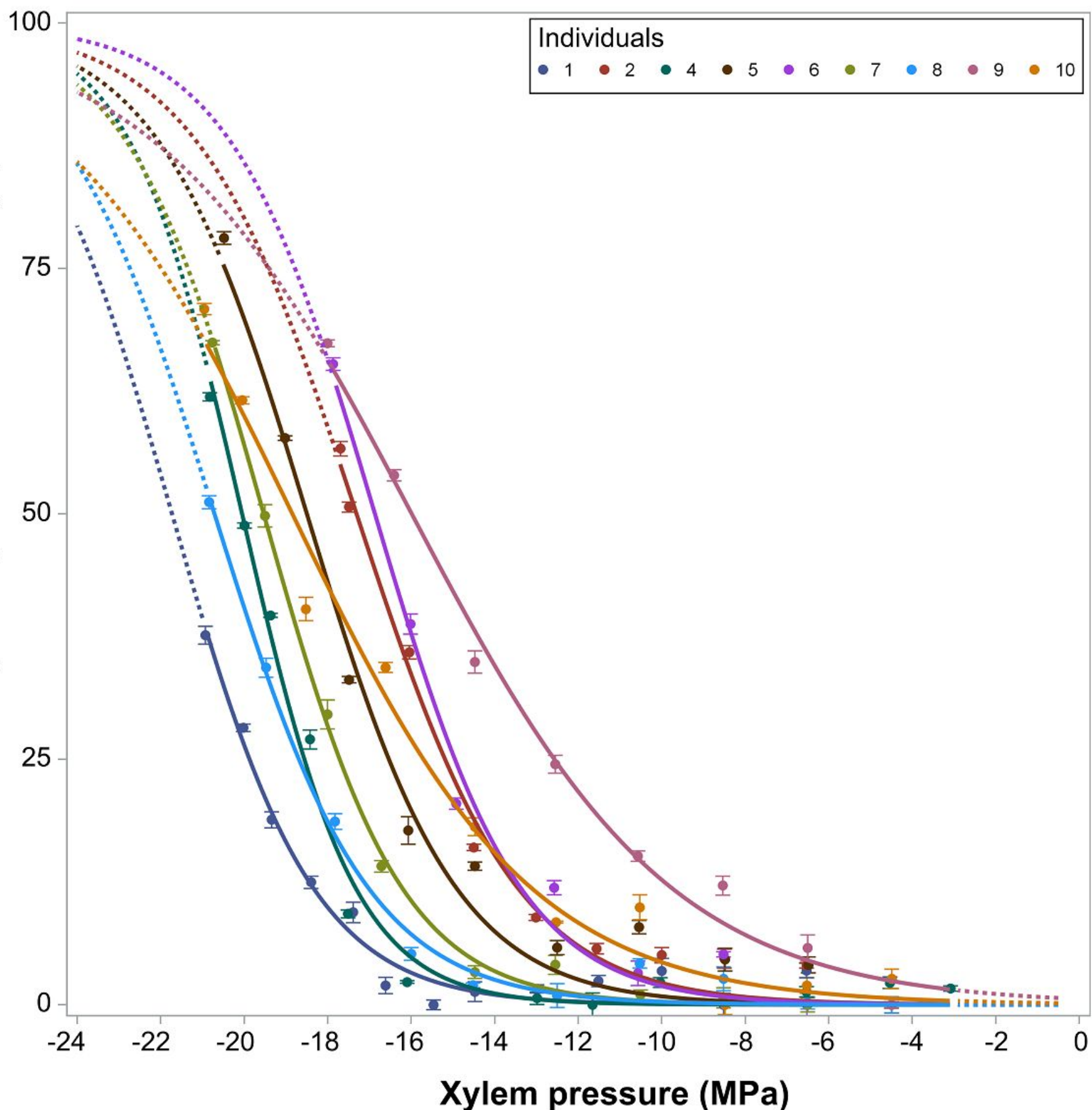
Figure S1. Climate diagram of average monthly precipitations and maximum temperatures for *Callitris tuberculata*'s estimated range. Black bars represent monthly precipitations, and the red curve shows maximum temperatures.

Figure S2. Vulnerability curves for nine individual trees of *Callitris tuberculata*. Each point represents mean value of percent loss of hydraulic conductance over at least three measurments of hydraulic conductance (bars represent ± standard error). Lines represent the Pammenter model fit to each individual curve, and dashed lines show were the model was expanded beyond experimental data.

Supplemental Table S1. Cavitation resistance parameters for each individual. P_{50}, P_{12} and P_{88} are respectively, the xylem pressure inducing 50%, 12% and 88% loss of xylem hydraulic conductance. S is the slope of the vulnerability curve at P_{50}. ks is the specific xylem conductivity, a standardized measurment of the samples' capacity to transport water.

Individual	P_{50} (MPa)	P_{12} (MPa)	P_{88} (MPa)	S (%.MPa^{-1})	ks (kg.m^{-1}.s^{-1}.MPa^{-1})
1	-21.73	-18.35	-25.11	14.80	0.000390
2	-17.31	-13.45	-21.17	12.96	0.000359
4	-20.05	-17.33	-22.76	18.42	0.000261
5	-18.50	-14.92	-22.07	13.99	0.000468
6	-16.87	-13.38	-20.35	14.34	0.000344
7	-19.53	-16.22	-22.84	15.10	0.000566
8	-20.71	-17.03	-24.39	13.58	0.000329
9	-15.99	-9.77	-22.20	8.04	0.000484
10	-18.85	-13.13	-24.56	8.75	0.000226
Average	-18.84	-14.84	-22.83	13.33	0.000381